Article:
Herrera-Abreu, MT, Pearson, A, Campbell, J et al. (2013) Parallel RNA interference screens identify EGFR activation as an escape mechanism in FGFR3-mutant cancer. Cancer Discovery, 3 (9). 1058 - 1071. ISSN: 2159-8274

https://doi.org/10.1158/2159-8290.CD-12-0569

Parallel RNA interference screens identify EGFR activation as an escape mechanism in *FGFR3* mutant cancer

Maria Teresa Herrera-Abreu[1], Alex Pearson[1], James Campbell[1], Stephen Shnyder[2], Margaret Knowles[3], Alan Ashworth[1], Nicholas C Turner[1,4]

1 The Breakthrough Breast Cancer Research Centre, Institute of Cancer Research, London, SW3 6JB, UK.

2 Institute of Cancer Therapeutics, University of Bradford, Richmond Road, Bradford BD7 1DP, UK

3 Section of Experimental Oncology, Leeds Institute of Molecular Medicine, St James's University Hospital, Leeds, LS9 7TF, UK

4 Breast Unit, Royal Marsden Hospital, Fulham Road, London, SW3 6JJ, UK

Corresponding author:

Nicholas Turner, The Institute of Cancer Research, 237 Fulham Road, London, SW3 6JB, UK, Fax: +44 (0) 207 51535340, Email: nicholas.turner@icr.ac.uk

Running title: FGFR driven cell line siRNA screens

Keywords: FGFR3, EGFR, siRNA screen, Bladder cancer

Financial support: M.H-A, A.A., N.T. were supported by Cancer Research UK (A10038).

Conflict of interest: We have no conflicts of interest

Word count: 4,953

Total no. of figures: 6 figures, 6 supplementary figures

Abstract (150 words)

Activation of the fibroblast growth factor receptors is a common oncogenic event. Little is known about determinants of sensitivity to FGFR inhibition and how this may differ between oncogenic FGFRs. Here through parallel RNA interference screens we demonstrate that EGFR mediates resistance to FGFR inhibition in *FGFR3* mutant cell lines, but not other *FGFR* driven cell lines. We describe two types of FGFR3 mutant cell lines: partially sensitive to FGFR inhibition, where inhibition of *FGFR3* results in transient down-regulation of MAPK signalling, which is rescued by rapid activation of EGFR signalling; and intrinsic resistant to FGFR inhibition, where EGFR dominates signalling through repression of FGFR3 expression, with EGFR inhibition rescued by delayed up-regulation of FGFR3 expression. Combinations of FGFR and EGFR inhibitors overcome this resistance mechanism *in vitro and in vivo*. Our results illustrate the power of parallel RNA interference screens in identifying common resistance mechanisms.

Statement of Significance (1-2 sentences)

Our data identifies a novel therapeutic approach to the treatment of *FGFR3* mutant cancer, suggesting that monotherapy targeting *FGFR3* is likely to have limited efficacy, emphasising the importance of exploring combination approaches to target both FGFR3 and EGFR. Our data emphasises the important role of EGFR in mediating resistance to inhibitors targeting a mutant oncogene, and that EGFR signalling can dominate the signalling from mutant *FGFR3.*

Introduction

Activating mutations of the FGF receptors are found in multiple cancer types, with the highest prevalence occurring with *FGFR3* mutations in bladder cancer(1) and *FGFR2* mutations in endometrial cancer(2, 3). In other cancer types activation predominantly occurs through amplification of the receptor, with *FGFR1* amplification in squamous

lung and breast cancer(4, 5), and *FGFR2* amplification in gastric and breast cancers(6, 7). Further mechanisms of activation include activating translocations involving the FGFRs, described initially in haematological malignancies although recently also described in solid tumours (8), and FGF ligand mediated signalling (9).

Preclinical studies have suggested that these oncogenic aberrations are potential therapeutic targets (2, 3, 6, 10-12), and multiple FGF receptors inhibitors have entered clinical trial with early evidence of efficacy with FGFR inhibitors in *FGFR1* amplified breast cancer (13, 14). Yet it is not clear what determines whether cancers will respond to FGFR inhibitors, what the mechanisms of resistance will be, and how this may differ between oncogenic receptors and cancer types. This presents a major limitation to the clinical development of FGFR inhibitors, and it is unclear which of the diverse mechanisms of activation of the FGF receptors are most likely to translate to clinical efficacy.

RNA interference (RNAi) screens have substantial potential in elucidating the determinants of sensitivity to cancer therapies (15-17), identifying both mechanisms of resistance (16) and key pathways that determine sensitivity (17). Here, we use parallel short interfering RNA (siRNA) screens to identify determinants of sensitivity and mechanisms of resistance to FGFR inhibition, in the protein kinome/phosphatome, along with a panel of amplified and mutant cancer cell lines to identify mechanisms specific to different *FGFR* mutation and amplifications. Through this approach we identify EGFR as a major factor limiting the efficacy of targeting *FGFR3* mutations.

Results

High-throughput Kinome/Phosphatome screens

To identify the determinants of sensitivity to FGFR inhibitors we conducted high-throughput parallel siRNA screens using a library targeting all known protein kinases and phosphatases and a panel of 11 *FGFR* amplified or mutant cell lines. Such parallel siRNA screens allow for comparison between different oncogenic aberrations, and have the potential to identify key mutation or subtype specific mechanisms of resistance (Figure 1A). The screening panel represented the most common *FGFR* aberrations observed in carcinomas, including cell lines with *FGFR1* amplification (JMSU1, H1581), *FGFR2* amplification (MFM223, SUM52, SNU16, KATOIII, OCUM2M), *FGFR2* mutation (AN3CA), and *FGFR3* mutation (*FGFR3* point mutated 97-7, MGHU3 and *FGFR3* translocated RT112M) (Figure 1B and Supplementary Table 1). Cell lines were transfected with the siRNA library in triplicate, and 48 hours later half of the plates were treated with the EC50 dose of the pan-FGFR inhibitor PD173074 and half with vehicle for 72 hours (Figure 1A). Vehicle control plates were used to examine for the effect of siRNA on cell survival/growth, and the relative growth in plates exposed to PD173074 versus vehicle was used to identify siRNA that altered sensitivity to PD173074 (Figure 1A).

Across the panel of *FGFR* driven cell lines, *FGFR1* amplified cell lines and *FGFR2* amplified/mutated cell lines were selectively sensitive to the corresponding siRNA, (Figure 1B), with in particular *FGFR2* amplified cell lines being strongly addicted to FGFR2. Similarly, across the panel of cell lines silencing of FGFR1 or FGFR2 was epistatic to FGFR inhibition in the corresponding cell lines (Supplementary Figure 1B). Unexpectedly a similar effect was not seen with FGFR3 siRNA in the *FGFR3* mutant cell lines, with FGFR3 siRNA having little or no effect on cell survival (Figure 1B). *FGFR3* cell lines were also noted to be relatively insensitive to PD173074 (Figure 1C), potentially suggesting the existence of alternative drivers of proliferation in the *FGFR3* mutant cell lines, and here we focus on the mechanisms of resistance in these cell lines.

EGFR is the key mediator of resistance in FGFR3 mutant cell lines

We set out to identify what determined sensitivity in *FGFR3* mutant cell lines and the factors that limited the sensitivity of these cell lines to FGFR inhibition. To identify features common to all three *FGFR3* mutant cell lines we performed supervised hierarchical clustering to identify the siRNA that differentially modulated sensitivity to PD173074 in *FGFR3* mutant cell lines compared to the other FGFR driven cell lines (Figure 1D). EGFR siRNA was the top siRNA that differentially increased sensitivity to PD173074 in the *FGFR3* mutant cell lines (Figure 1D). EGFR siRNA sensitised all three of the *FGFR3* mutant bladder cell lines screened to PD173074, but none of the other cell lines, identifying a clear subtype/mutation specific event (Figure 1E). EGFR siRNA also reduced the survival of the PD173074 insensitive 97-7 cell line, suggesting that this cell line may be primarily EGFR dependent (Figure 1E). The effect of EGFR on sensitivity to PD173074 was validated with two independent siRNA targeting EGFR (Figure 2A), and the selectivity of the effect to *FGFR3* mutant cell lines was also confirmed with EGFR inhibitors in short term survival assays (Supplementary Figure 2A). Therefore, through the use of parallel siRNA screens we identified a common subgroup specific resistant mechanism (Figure 1 and Supplementary Figure 1)

To understand why EGFR siRNA appeared to sensitise only *FGFR3* mutant cell lines, we examined EGFR expression and phosphorylation by western blotting. The *FGFR3* mutant bladder cancer cell lines expressed high levels of both total and phosphorylated EGFR (Figure 2C), with EGFR not phosphorylated in the other cell lines. *FGFR3* mutant bladder cancer cell lines expressed high levels of TGFα suggesting a potential autocrine loop. We performed clonogenic assays in the *FGFR3* mutant cell lines to further examine the potential role of EGFR in these cell lines. Colony formation was either abolished, or substantially decreased, by the

combination of PD173074 and gefitinib (Figure 2D), and by combinations of cetuximab and PD173074 (Supplementary Figure 2C). To confirm that this observation extended beyond the cell lines used in the screen, we treated additional *FGFR3* point mutant cell lines, again with substantial combination efficacy in 94-10 and 639V (Figure 2D).

Two distinct patterns of response to PD173074 and gefitinib were apparent in the clonogenic and short-term survival assays (Figure 2D, Figure 1C and Supplementary Figure 2A and B). The RT112M, MGHU3, and 639V cell lines were partially FGFR dependent: PD173074 modestly reduced colony formation although combination with the EGFR inhibitor gefitinib further reduced clonogenic survival, suggesting that in these cell lines EGFR limited sensitivity to FGFR inhibition. In contrast, the 97-7 and 94-10 cell lines were principally EGFR dependent: Gefitinib alone susbstantially reduced colony formation with PD173074 alone having no effect on the growth of these cell lines, suggesting that EGFR mediated the intrinsic resistance of these cell lines to PD170374. In the presence of gefitinib, clonogenic survival was further reduced by PD173074, suggesting that reciprocally in 97.7 and 94.10 FGFR limited sensitivity to EGFR inhibition.

In both 97-7 and RT112M combined inhibition of FGFR and EGFR, with PD173074 and gefitinib, induced a greater loss of S phase compared to either inhibitor given alone (Figure 2E and Supplementary Figure 3B), concomitant with a relatively increased p27 levels with the combination (Figure 2F). This suggested that the combined effect of the inhibitors was mediated predominantly through greater cell cycle arrest. Although we did observe that gefitinib and in particular the combination, increased PARP cleavage in 97-7 (Figure 2F).

Therefore, we identified that EGFR mediated resistance to FGFR3 targeting in all five *FGFR3* mutant cell lines examined. We described two groups of *FGFR3* mutant cell lines, with one group partially *FGFR3* dependent due to EGFR signalling limiting sensitivity to FGFR inhibitors, and the other group primarily EGFR dependent although in these cell lines FGFR3 limited sensitivity to EGFR inhibition.

Inhibition of FGFR3 results in upregulation of EGFR signalling in partially FGFR3 dependent cell lines

We investigated the link between EGFR and FGFR3 signalling in these cell lines, how one receptor compensated for inhibition of the alternative receptor, and whether the same mechanisms where involved in the partially FGFR3 dependent and EGFR dependent cell lines.

We first focused on the cell lines that were partially FGFR3 dependent. In the RT112M and 639V cell lines PD173074 completely suppressed ERK1/2 phosphorylation at 1 hour, confirming the FGFR3 was the dominant receptor in these cell line (Figures 3A). However, at later time points ERK1/2 phosphorylation was partially restored, reaching steady state by 4 hours. The increase in ERK1/2 phosphorylation was accompanied by upregulated EGFR Tyr1068 phosphorylation (Figure 3A). A similar pattern was also seen in the PD173074 sensitive MGHU3 cell line (Supplementary Figure 3A). The restoration of ERK1/2 phosphorylation was blocked by the addition of gefitinib both at 6 hours and chronically at 24 hours (Figure 3B). To ascertain whether the reactivation of MAPK signalling explained the relative insensitivity to FGFR inhibition, we examined the combination of PD173074 and the MEK inhibitor CI-1040. In RT-112M cells, CI-1040 increased sensitivity to PD170374 in clonogenic assays suggesting that in part reactivation of MEK-ERK1/2 signalling by EGFR induced resistance to PD173074 (Figure 3C). Therefore our results suggest that up-regulation of EGFR signalling promoted restoration of MAPK

signalling and ERK1/2 phosphorylation that compensated for the loss of FGFR signalling induced by PD173074.

We noted that AKT-Ser473 phosphorylation was unaltered by PD173074 in both RT112M and 639V, suggesting that FGFR3 may signal relatively weakly through PI3 kinase. Consistent with the relatively limited effect of PD173074 on down-stream signalling in these cell lines, PD1730743 induced a cytostatic effect (Figures 2E and 2F, and Supplementary Figure 3B). The combination of PD173074 with gefitinib lead to greater suppression of AKT-Ser473 phosphorylation in RT112M (Figure 3D), which suggest that the combination suppressed multiple down-stream signalling pathways.

Mechanism of EGFR activation by FGFR inhibitors

We set out to establish how EGFR signalling was upregulated by FGFR3 inhibition.

In the EGFR dependent cell lines 97-7 and 94-10, PD170374 had no effect on down-stream signalling and no effect of EGFR phosphorylation (Figure 3D), suggesting that the upregulation of EGFR seen with PD173074 in FGFR3 dependent cell lines did not reflect FGFR inhibition *per se*, but the resulting loss of down stream signalling. We hypothesised that the decrease in ERK1/2 activity that occurred with PD173074, resulted in the upregulation of EGFR signalling (Figure 3A). Multiple mechanisms of regulation of EGFR signalling through negative feedback loops mediated by MEK-ERK1/2 signalling have been described, such as the ERK1/2 mediated phosphorylation of CBL to promote receptor internalisation and degradation, and to promote expression of the sprouty proteins (18). Indeed Inhibition of MEK with CI-1040 in RT112M cells decreased ERK1/2 phosphorylation and substantially upregulated EGFR Tyr1068 phosphorylation (Figure 4A). This therefore suggested a model whereby FGFR3 mediated MAPK signalling suppressed signalling from EGFR, and that this negative feedback was subsequently

released by FGFR3 inhibition leading to de-repressed EGFR signalling. In keeping with this model EGFR was phosphorylated at substantially lower levels in the cell lines where FGFR3 signalling predominated (RT112M and MGHU3) compared to 97-7 where EGFR signalling was dominant (Figure 2D).

We examined for other potential mechanisms relevant to the FGFR3-EGFR feedback. The *FGFR3* mutant bladder cancer cell lines expressed high levels of autocrine TGFα, although TGFα expression was unaltered by FGFR inhibition suggesting that upregulation of ligand did not explain upregulated EGFR signalling (Figure 4B). We were unable to demonstrate co-immunoprecipiation between EGFR and FGFR3 suggesting that the two receptors did not interact (Supplementary Figure 3C). The CDC25 familly has been identified as a potential EGFR phosphatase (19), and has previously been suggested to mediate a feedback loop between inhibition of mutant BRAF and EGFR (16)(20). Silencing CDC25C with multiple different siRNA increased EGFR phosphorylation and downstream signalling (Supplementary Figure 4B). However, we were unable to demonstrate a decrease in CDC25C-Thr48 phosphorylation with PD170374 in RT112M cells, the site proposed to be regulated by ERK1/2 (20), (Supplementary Figure 4C), suggesting that although CDC25C is a phosphatase that regulates EGFR phosphorylation and signalling (Supplementary Figure 4), it was unlikely to be involved in the feedback upregulation mediated by PD173074 in these cell lines. Moreover, the siRNA against CDC25C did not affect sensitivity to PD173074 in either RT112M or MGHU3 (Supplementary Figure 4A).

Receptor internalisation and trafficking is a major factor regulating the signalling from receptor tyrosine kinases, with internalisation ultimately leading to signal termination (18). After internalisation, EGFR continues to signal from early endosomes with signalling only terminated later due to subsequent lysosomal degradation, or in late recycling endosomes (18). To examine if there was a defect in receptor trafficking

that may contribute to EGFR upregulation we examined EGFR location by immunofluoresnce. In RT112M cells, PD173074 treatment led to EGFR accumulating at the plasma membrane, in regions characterised by aberrant dense cortical filamentous actin (F-actin) (Figure 4C), and in giant early endosomes (Figure 4D and E). This suggested that the activation of EGFR following FGFR inhibition was multifactorial, mediated by both loss of negative feedback and subsequent impaired receptor internalisation and sorting of receptor that would contribute through impaired signalling termination.

FGFR3 mediates resistance to EGFR targeting through transcriptional upregulation of FGFR3 expression

We next focused on the cell lines that were primarily EGFR dependent, to understand why these cell lines were EGFR dependent and how following EGFR inhibition the cells became FGFR dependent (Figure 2D and supplementary Figure 2A and B). In the EGFR dependent cell lines 97-10 and 94-10 gefitinib acutely blocked both ERK1/2 and AKT-Ser473 phosphorylation confirming that EGFR dominated down stream signalling in these cell lines. Gefitinib alone had no effect on signalling in the FGFR3 dependent cell lines (Figure 5A), an inverse of the effect seen with PD173074 (Figure 3A). Therefore, in any one cell line either FGFR3 or EGFR was the dominant receptor controlling signalling, and this directly reflected the sensitivity to the corresponding inhibitor.

Whereas in the FGFR3 dependent cell lines PD173074 lead to relatively rapid upregulation of EGFR and restoration of ERK1/2 phosphorylation (Figure 3), in the EGFR dependent cell lines the restoration of ERK1/2 phosphorylation was much delayed only occuring after 24 hours exposure to PD173074 (Figure 5A and 5C). The delayed restoration of ERK1/2 phosphorylation was blocked by PD173074

(Figure 5B and 5C), confirming that in these cell lines FGFR signalling compensated for the loss of EGFR signalling.

The very substantial difference in the kinetics of the restoration of downstream signalling by the non-dominant EGFR/FGFR3 receptor (Figure 3A and 5A) suggested that the mechanism(s) leading to upregulation of FGFR3 signalling were distinct. Concurrent with the increase in ERK1/2 phosphorylation we observed substantial upregulation of FGFR3 protein, in particular the fully glycosylated form (Figure 5A), and upregulated FRS2 phosphorylation (adapter protein of FGFRs, Figure 5D). Gefitinib lead to substantial increased FGFR3 mRNA transcription in the EGFR dependent 97-7 cell lines (Figure 5E), with the increase in transcription seen not at 6 hours but at 24 hours mirroring the timing of increased FGFR3 (Figure 5A).

Therefore, these data demonstrated that EGFR signalling suppressed FGFR3 transcription, and gefitinib released this suppression resulting in restoration of FGFR3 expression and signalling. Similar to that observed with EGFR, FGFR3 also accumulated in the cytoplasmic membrane after gefitinib treatment (Figure 5F), whereas in untreated cells FGFR3 was predominantly cytoplasmic, suggesting that upregulation of FGFR3 was also reinforced by impaired receptor internalisation. In the EGFR dominant cell lines, EGFR was expressed at higher levels relative to FGFR3 (Figure 2C, and Figure 5G and H), suggesting that EGFR dominated in these cell lines through suppression of FGFR3 expression.

Together, these data suggest a model whereby FGFR3 is activated in *FGFR3* mutant cell lines, although EGFR is also activated through autocrine ligand expression. In steady state one receptor dominated downstream signalling, this being FGFR3 in RT112M, MGHU3 and 639V, and EGFR in 97-7 and 94-10 cells. Inhibition of the dominant receptor released negative feedback repression, although with distinct

mechanisms between EGFR and FGFR3, that promotes signalling from the alternative receptor and this drive inhibitor resistance.

In vivo efficacy of combined EGFR and FGFR inhibition

We established xenografts of RT112M cells in nude mice to examine efficacy *in vivo.* The combination of gefitinib and PD173074 was poorly tolerated at the doses used with rapid weight loss (Supplementary Figure 5). Nevertheless, the short duration of 3 days combination therapy reduced tumour volume to a greater extent than either treatment given alone, including two complete responses (Figure 6A), confirming that the *in vitro* observations predicted for greater tumour control with combination treatment *in vivo.*

We repeated experiments with the combination of cetuximab and PD173074 given for two weeks of treatment, which was well tolerated (Supplementary figure 5). The combination of cetuximab and PD173074 reduced tumour size to a significantly greater extent than either agent given alone ($p<0.0001$ Log-Rank test, Figure 6B). Treatment with PD173074 lead to tumour stasis whereas combination therapy lead to substantial tumour reduction (mean relative tumour volume at end of 2 week treatment period 1.28 PD173074 vs 0.51 combination, $p=0.006$ Student's T-test). On stopping treatment PD173074 tumours rapidly resumed growth, whereas the combination treated animals had sustained tumour control (median time to tumour doubling control 6 days, cetuximab 13 days, PD173074 17 days, combination group median not reached after 41 days follow-up, Figure 6C). These dated suggested substantial synergistic efficacy *in vivo* between dual targeting of EGFR and FGFR3 to *FGFR3* mutant cell lines.

Discussion

In this study we have utilized parallel RNA interference screens in multiple FGFR dependent cell lines to dissect mechanisms of resistance to FGFR inhibition. We show that the sensitivity of *FGFR3* mutant cancers is limited by intrinsic activation of EGFR in these cell lines. We described two groups of cell lines. In partially FGFR3 dependent cell lines, EGFR signalling is upregulated following FGFR inhibition through release from negative feedback, and this compensates for loss of FGFR signalling. In EGFR dependent cell lines, despite the presence of an activating *FGFR3* mutation, EGFR dominates down-stream signalling. This in part reflected that *FGFR3* is a relatively weak oncogenic signal, and in addition that EGFR signalling inhibited FGFR3 transcription. In these cell lines inhibition of EGFR resulted in upregulated FGFR3 expression that restored FGFR3 signalling, and compensated for loss of EGFR signalling.

FGFR3 mutation is one of the most common oncogenes in transitional cell carcinomas of the bladder, also described at relatively high frequency in cervical cancer and squamous cell carcinomas of the upper aero-digestive tract (1). Recent data has confirmed that *FGFR3* is also activated by translocation in cancer, generating fusion protein of *FGFR3* fused at the c-terminus deleting the last exon of *FGFR3* to a number of partner proteins, in glioblastoma (21) and bladder cancer(22). Our observations suggest that FGFR inhibitor mono-therapy is likely to have relatively limited efficacy in *FGFR3* mutant cancer, and advises combination therapeutic approaches with EGFR targeting therapies. The RT112M cell line has an activating translocation of FGFR3(22), suggesting that limited efficacy may also be seen in targeting *FGFR3* translocations.

We demonstrate a reciprocal relationship between targeting the dominant oncogene and rescue mediated by an alternative receptor tyrosine kinase, which is emerging as a major mechanism of resistance to cancer therapies (23-26). We demonstrate

that this can extend further to independence from the oncogene for signalling, when an oncogene such as FGFR3 is relatively weak. We provide evidence that the mechanism of rescue by receptor tyrosine kinase differs between rescue by FGFR3 and EGFR. In FGFR3 dependent cell lines, EGFR signalling is upregulated relatively rapidly following loss of MAPK signalling negative feedback induced by PD173074, and consequently PD173074 has only minor effects on clonogenic survival (Figure 2D). FGFR inhibition in *FGFR3* mutant cell lines did not induce an apoptotic response (Figure 2F and Supplementary Figure 3). Such a cytostatic response allows for upregulation of the alternative receptor to subvert the effect of inhibition of the dominant receptor. In contrast, in EGFR dependent cell lines rescue by EGFR is reliant on delayed upregulation of FGFR3 expression. The substantial sensitivity seen with gefitnib alone in EGFR dependent cell lines suggested that the rescue by FGFR3 is less efficient than the reciprocal rescue by EGFR (Figure 2D). Therefore, the relative inefficiency of rescue by FGFR3 may reflect both the delay in FGFR3 upregulation and the more dominant effect of gefitinib of down-stream signalling (Figure 5A).

Impaired receptor trafficking likely re-inforces the upregulation of both receptors. In response to FGFR3 inhibition, EGFR accumulates at the membrane and in early endosomes, and likewise in response to EGFR inhibition FGFR3 accumulates at the membrane. Although internalization was initially thought to trigger signal termination, it is now clear that tyrosine kinase receptors signal from early endosomes, with signal termination occurring only later in trafficking during lysosomal degradation or in recycling endosomes (18). FGFR3 and EGFR was noted to accumulate at the membrane in areas of abnormally dense actin filament formation, and it will be interesting in future research to examine the possible role of aberrant regulation of the cytoskeleton in receptor accumulation (27).

We demonstrate that in all *FGFR3* mutant bladder cancer cell lines EGFR is also active, yet in any single cell line at steady state only one receptor controls down-stream signalling. The surprising observation is that in some cell lines EGFR is the dominant receptor. The observation that EGFR signalling suppresses FGFR3 expression combined with the higher EGFR expression in EGFR dependent cell lines (Figure 5F), potentially suggest that at some point in tumour development EGFR expression rose to a level where it suppressed FGFR3 expression and dominated down-stream signalling. EGFR is also shown to be more pleotropic in signalling than FGFR3. Whereas in the FGFR3 dependent cell lines PD173074 has no effect on PI3K-AKT signalling (Figure 3A), in the EGFR dependent cell lines gefitinib substantially reduced PI3K-AKT signalling (Figure 5A). Therefore mutated *FGFR3* could likely be seen as a relatively weak oncogene, that can be subverted by more dominant EGFR signalling.

The clinical translational challenge in tackling the upregulation of receptor tyrosine kinases in mediating resistance to targeted therapies is the identification of the receptor that drives resistance to targeting cancer. Our data partially overcomes this challenge for *FGFR3* mutant bladder cancer by demonstrating that EGFR is active and mediates resistance in all five *FGFR3* cell lines examined. The MET receptor has also been shown to be an important receptor mediating resistance, potentially through both paracrine stromal release (23) or autocrine production of HFG ligand (28). Our results are potentially conflicting with recent data that potentially suggested MET as the mediator of resistance to FGFR3 targeting in RT112M (23, 28). However, we show that EGFR is the receptor that compensates for FGFR inhibition, and that this translates to substantial combination efficacy *in vivo* (Figure 6). Examining a publically available gene expression series we find that TGFA mRNA is expressed at high levels in bladder cancer (Figure 6C), whereas HGF mRNA is expressed at low levels (Supplementary Figure 6), suggesting that our observations

may be clinically relevant. Our data is also consistent with the recently identified role of EGFR in mediating resistance to mutant *BRAF* targeting in colon cancer (16, 24).

Our results do suggest caution in the combination of FGFR and EGFR inhibitors, with the combination of PD173074 and gefitinib poorly tolerated in mice at the doses used (Supplementary Figure 5). The combination of PD173074 and the EGFR inhibitory antibody cetuximab had improved tolerance (Supplementary Figure 5), suggesting that the improved specificity of monoclonal antibodies partially mitigate the toxicity. FGFR therapeutic antibodies that further maximize specificity (29, 30) and further mitigate toxicity associated with broader FGFR family inhibition that occurs with tyrosine kinase inhibitors. Relatively limited efficacy has been observed with EGFR family inhibition in bladder cancer (31). Our data showing that upregulation of FGFR3 signalling mediates resistance to EGFR targeting, may potentially explain this relative lack of efficacy, providing a further rational to develop the combination in bladder cancer.

Our study illustrates the power of parallel RNA interference screens to identify key determinants of resistance to targeted therapies. Through simultaneous examination of multiple cell lines with related oncogenic aberrations, the key common determinants of sensitivity can be identified, which may remain obscured by the multiplicity of effects and noise seen in any one individual screen (Supplementary Figure 1C). This approach could be applied to multiple different targeted therapies to identify the key determinants of sensitivity and reveal the common shared mechanisms of resistance.

Methods

Cell lines and antibodies

Bladder cells lines (RT112M, MGHU3, 639V, 97.7, 94.10) were from the laboratory of MA Knowles (12). Other cell lines were obtained from ATCC or Asterand. Cell lines were banked in multiple aliquots on receipt to reduce risk of phenotypic drift, and identity confirmed by STR profiling with the PowerPlex 1.2 System (Promega). Cell lines were maintained in phenol red free DMEM, DMEM/F12, or RPMI with 10% FBS (PAA gold) and 2mM L-glutamine (Sigma-Aldrich, Dorset, UK). Antibodies used were phosphorylated AKT-Ser473 (4058), AKT (4691), phospho-ERK1/2-Thr202/Tyr204 (4370), EGFR (2232), phospho-EGFR-tyr 1068 (3777), phospho-CDC25C-Thr48 (9527) (all Cell Signalling Technology, Danvers, MA), β-actin (A5441) (Sigma), FGFR3 (sc-13121), EGFR (sc-03), TGFα (sc-374433), p27 (sc-528), PARP (sc-7150), FRS2 (sc-8318) (Santa-Cruz Biotechnology, Santa Cruz, CA). PD173074 was from Sigma, gefitinib from Tocris, and CI-1040 from Selleckchem.

siRNA screening

Screening was in 384 well plates with a Dharmacon siGENOME SMARTpools library targeting all known protein kinases and phosphatases essentially as described previously (17, 32). Briefly, cells were reverse transfected at final siRNA concentration 20nM, at 48 hours post transfection half the plates were treated with PD173074 at the EC50 and half vehicle, and survival was assessed after 72 hours exposure with Cell Titre-Glo cell viability assay (Promega, Madison, WI). Individual plates were median normalised before combination. The siRNA library was supplemented with non-targeting siRNA, PLK1 siRNA as a viability control, and 4 individual siRNA against the FGFR1-4 receptor family (Supplementary Table 2). Screens were only accepted with a Z' factor >0.3.

To assess the effect of siRNA on growth/survival, the effect of siRNA in the vehicle plates was expressed as a Z score, with the standard deviation estimated from the median absolute deviation (MAD). A Z score of <-2, approximately the 95%

confidence intervals, was considered evidence of a significant decrease in survival with siRNA.

To assess the effect of siRNA on sensitivity to PD173074 the log2 ratio between growth in PD173074 plates and vehicle plates was assessed and expressed as a Z score. A Z score of <-1.645 was considered evidence of increased sensitivity to PD170374, and >1.645 as relative resistance (cut-offs equivalent to putative 90% confidence intervals). A lower cut-off was used for sensitivity score to reflect that multiple siRNA altered sensitivity, affecting the null hypothesis in assessment of the standard deviation from the MAD, and clear evidence that reproducible effects were seen with siRNA using this cut-off (Supplementary Figure 1).

In vitro cell line assessment

Clonogenic assays were conduced in 6 well plates, with 1000-2000 cells seeded per well, and 24 hours later cells exposed to 500 nM PD173074, 250 nM Gefitinib, or the combination, followed by growth in media for 2 weeks to allow colony growth. Colonies were fixed, stained with sulforhodamine B, and counted. For short-term survival assays, cells were exposed to fixed-ratio combinations of PD173074 and Gefitinib, and survival was assessed after 72 hours exposure with Cell Titre-Glo cell viability assay (Promega, Madison, WI). For EGFR siRNA short-term survival assays RT112M cells were reverse transfected at final siRNA concentration 20nM, at 48 hours post transfection plates were treated with PD173074 at the EC50 or vehicle, and survival was assessed after 72 hours exposure.

siRNA Data analysis

To compare siRNA results between two groups, we used supervised methods calculating the difference in the median effect of the siRNAs between the 2 groups, followed by estimation of a p value by permutation of labels to create a distribution

for comparison with the actually differences (32). A significance cut-off of $p < 0.05$ was used.

Western blotting and FACS

Cell lines where grown on 35mm plates, treated as indicated, and lysed in NP40 lysis buffer. Western blots were carried out with precast TA or Bis-Tris gels (Invitrogen) as previously described. FACS analysis was performed as previously described (35).

Immunofluorescence

Cells grown on coverslips were fixed with 4% paraformaldehyde, before incubation with primary antibodies against EGFR (1:100, sc-03), FGFR3 (1:100, sc-13121) EEA1 (1:1000, sc-33585) (Santa-Cruz Biotechnology, Santa Cruz, CA), Alexa-488 phalloidin (1:1000, A12379) (Invitrogen), and corresponding secondary Alexa-444 or Alexa-555 conjugates antibodies, with DAPI nuclear stain. Cells were visualized with a Leica Confocal microscope.

Quantitative PCR

cDNA was synthesised from RNA using Superscript III and random hexamers (Invitrogen). Quantitative PCR was performed by absolute quantification with TAQMAN chemistry on an ABI Prism 7900T System (Applied Biosystems) for FGFR3 (Hs00997 400) and expressed relative to control gene GAPDH (Hs 02758991).

Xenografts

RT112M xenografts in nude mice were generated by transplantation as previously described (12). In the first experiement mice were treated with PD173074 20mg/kg by intraperitoneal injection, gefitinib 100mg/kg by oral gavage, or the combination, for 3 days. In the second experiment mice were treated with PD173074 15mg/kg on

days 0-3 and 7-10, cetuximab 40mg/kg day 0 day 3 day 7 and day 10 , or the combination by intraperitoneal injection. Tumour size was assessed at least three times a week. Time to tumour doubling was assessed by Kaplan-Meier methods as either doubling of relative tumour volume or tumour ulceration, censoring mice lost to follow-up through reasons not related to tumour progression.

Statistical analysis

All statistical tests were performed with GraphPad Prism version 5.0 or Microsoft Excel. Unless stated otherwise, p values were two tailed and considered significant if $p<0.05$. Error bars represent SEM of three experiments. Normalised gene expression data assessed on Affymetrix Human Genome U133A Arrays from Sanchez-Carbayo et al were downloaded as log2 median centered data with probe 205016_at for TGFA from www.oncomine.org (36).

Acknowledgements

We thank Christopher Marshall for discussion and advice on the data. This work was supported by grants from Cancer Research UK. Dr Nicholas Turner is a CRUK Clinician Scientist. We acknowledge NHS funding to the NIHR Biomedical Research Centre.

References

1. Cappellen D, De Oliveira C, Ricol D, et al. Frequent activating mutations of FGFR3 in human bladder and cervix carcinomas. Nat Genet 1999; 23: 18-20.

2. Pollock PM, Gartside MG, Dejeza LC, et al. Frequent activating FGFR2 mutations in endometrial carcinomas parallel germline mutations associated with craniosynostosis and skeletal dysplasia syndromes. Oncogene 2007; 26: 7158-62.

3. Dutt A, Salvesen HB, Chen TH, et al. Drug-sensitive FGFR2 mutations in endometrial carcinoma. Proc Natl Acad Sci U S A 2008; 105: 8713-7.

4. Courjal F, Cuny M, Simony-Lafontaine J, et al. Mapping of DNA amplifications at 15 chromosomal localizations in 1875 breast tumors: definition of phenotypic groups. Cancer Res 1997; 57: 4360-7.

5. Weiss J, Sos ML, Seidel D, et al. Frequent and focal FGFR1 amplification associates with therapeutically tractable FGFR1 dependency in squamous cell lung cancer. Sci Transl Med 2010; 2: 62ra93.

6. Kunii K, Davis L, Gorenstein J, et al. FGFR2-amplified gastric cancer cell lines require FGFR2 and Erbb3 signaling for growth and survival. Cancer Res 2008; 68: 2340-8.

7. Heiskanen M, Kononen J, Barlund M, et al. CGH, cDNA and tissue microarray analyses implicate FGFR2 amplification in a small subset of breast tumors. Anal Cell Pathol 2001; 22: 229-34.

8. Singh D, Chan JM, Zoppoli P, et al. Transforming Fusions of FGFR and TACC Genes in Human Glioblastoma. Science 2012.

9. Turner N, Grose R. Fibroblast growth factor signalling: from development to cancer. Nat Rev Cancer 2010; 10: 116-29.

10. Turner N, Lambros MB, Horlings HM, et al. Integrative molecular profiling of triple negative breast cancers identifies amplicon drivers and potential therapeutic targets. Oncogene 2010; 29: 2013-23.

11. Tannheimer SL, Rehemtulla A, Ethier SP. Characterization of fibroblast growth factor receptor 2 overexpression in the human breast cancer cell line SUM-52PE. Breast Cancer Res 2000; 2: 311-20.

12. Lamont FR, Tomlinson DC, Cooper PA, Shnyder SD, Chester JD, Knowles MA. Small molecule FGF receptor inhibitors block FGFR-dependent urothelial carcinoma growth in vitro and in vivo. Br J Cancer 2011; 104: 75-82.

13. Andre F, Bachelot TD, Campone M, et al. A multicenter, open-label phase II trial of dovitinib, an FGFR1 inhibitor, in FGFR1 amplified and non-amplified metastatic breast cancer. J Clin Oncol 2012; 29.

14. Soria JC, Dienstmann R, de Braud F, et al. FIRST-IN-MAN STUDY OF E-3810, A NOVEL VEGFR AND FGFR INHIBITOR, IN PATIENTS WITH ADVANCED SOLID TUMORS. Annals of Oncology 2012; 23: L2.5.

15. Berns K, Horlings HM, Hennessy BT, et al. A functional genetic approach identifies the PI3K pathway as a major determinant of trastuzumab resistance in breast cancer. Cancer Cell 2007; 12: 395-402.

16. Prahallad A, Sun C, Huang S, et al. Unresponsiveness of colon cancer to BRAF(V600E) inhibition through feedback activation of EGFR. Nature 2012; 483: 100-3.

17. Turner NC, Lord CJ, Iorns E, et al. A synthetic lethal siRNA screen identifying genes mediating sensitivity to a PARP inhibitor. EMBO J 2008; 27: 1368-77.

18. Avraham R, Yarden Y. Feedback regulation of EGFR signalling: decision making by early and delayed loops. Nat Rev Mol Cell Biol 2011; 12: 104-17.

19. Wang Z, Wang M, Lazo JS, Carr BI. Identification of epidermal growth factor receptor as a target of Cdc25A protein phosphatase. J Biol Chem 2002; 277: 19470-5.

20. Wang R, He G, Nelman-Gonzalez M, et al. Regulation of Cdc25C by ERK-MAP kinases during the G2/M transition. Cell 2007; 128: 1119-32.

21. Singh D, Chan JM, Zoppoli P, et al. Transforming fusions of FGFR and TACC genes in human glioblastoma. Science 2012; 337: 1231-5.

22. Williams SV, Hurst CD, Knowles MA. Oncogenic FGFR3 gene fusions in bladder cancer. Hum Mol Genet 2012.

23. Wilson TR, Fridlyand J, Yan Y, et al. Widespread potential for growth-factor-driven resistance to anticancer kinase inhibitors. Nature 2012; 487: 505-9.

24. Corcoran RB, Ebi H, Turke AB, et al. EGFR-mediated re-activation of MAPK signaling contributes to insensitivity of BRAF mutant colorectal cancers to RAF inhibition with vemurafenib. Cancer Discov 2012; 2: 227-35.

25. Garofalo M, Romano G, Di Leva G, et al. EGFR and MET receptor tyrosine kinase-altered microRNA expression induces tumorigenesis and gefitinib resistance in lung cancers. Nat Med 2011; 18: 74-82.

26. Straussman R, Morikawa T, Shee K, et al. Tumour micro-environment elicits innate resistance to RAF inhibitors through HGF secretion. Nature 2012; 487: 500-4.

27. Wang W, Eddy R, Condeelis J. The cofilin pathway in breast cancer invasion and metastasis. Nat Rev Cancer 2007; 7: 429-40.

28. Harbinski F, Craig VJ, Sanghavi S, et al. Rescue screens with secreted proteins reveal compensatory potential of receptor tyrosine kinases in driving cancer growth. Cancer Discov 2012; 2: 948-59.

29. Qing J, Du X, Chen Y, et al. Antibody-based targeting of FGFR3 in bladder carcinoma and t(4;14)-positive multiple myeloma in mice. J Clin Invest 2009; 119: 1216-29.

30. Trudel S, Stewart AK, Rom E, et al. The inhibitory anti-FGFR3 antibody, PRO-001, is cytotoxic to t(4;14) multiple myeloma cells. Blood 2006; 107: 4039-46.

31. Wulfing C, Machiels JP, Richel DJ, et al. A single-arm, multicenter, open-label phase 2 study of lapatinib as the second-line treatment of patients with locally advanced or metastatic transitional cell carcinoma. Cancer 2009; 115: 2881-90.

32. Brough R, Frankum JR, Sims D, et al. Functional viability profiles of breast cancer. Cancer Discov 2011; 1: 260-73.

33. Chou TC, Talalay P. Quantitative analysis of dose-effect relationships: the combined effects of multiple drugs or enzyme inhibitors. Advances in enzyme regulation 1984; 22: 27-55.

34. Wu G, Feng X, Stein L. A human functional protein interaction network and its application to cancer data analysis. Genome Biol 2010; 11: R53.

35. Turner N, Pearson A, Sharpe R, et al. FGFR1 amplification drives endocrine therapy resistance and is a therapeutic target in breast cancer. Cancer Res 2010; 70: 2085-94.

36. Sanchez-Carbayo M, Socci ND, Lozano J, Saint F, Cordon-Cardo C. Defining molecular profiles of poor outcome in patients with invasive bladder cancer using oligonucleotide microarrays. J Clin Oncol 2006; 24: 778-89.

Figure legends

Figure 1. High-throughput siRNA Kinome/Phosphatome to identify genes required for the growth of *FGFR* amplified and mutant cell lines and sensitivity to FGFR inhibition.

A. Schematic of siRNA screen. Cells were reverse transfected in 384 well plates with siRNA SMARTpools targeting all known protein kinases and phosphatases, and 48 hours later exposed to PD170374 at EC50, or control, and survival assessed after 72 hours exposure. The effect of siRNA on survival was assessed on the vehicle plates (Survival effect), and the effect of siRNA on sensitivity to PD173073 was assessed as the relative growth in PD173074 plates compared to vehicle (Sensitivity to PD173074). Both analyses were expressed as a Z score.

B. Survival effect of FGFR1, FGFR2, and FGFR3 siRNA according to *FGFR* gene mutation/amplification; left *FGFR1* amplified, centre *FGFR3* mutation, right *FGFR2* amplified and mutated (AN3CA). Black bars indicate those siRNA with a significant effect in cell survival, defined as a Z score <-2.

C. Relative growth of the panel of screened cell lines to a range of concentration of PD173074.

D. Supervised clustering of the siRNA effect on sensitivity to PD173074, with the differential effect of siRNA according to *FGFR3* mutational status. Displayed are siRNA with a permutation p value <0.05 ordered by mean effect in the *FGFR3* mutant cell lines.

E. *Top.* EGFR siRNA increased sensitivity to PD173073 specifically in *FGFR3* mutant cell lines, p=0.001 Student's T test. *Bottom.* Survival effect of EGFR siRNA. EGFR siRNA significantly reduced the survival of the 97-7 cell line.

Figure 2. EGFR is intrinsically active in *FGFR3* mutant lines and combined targeting of EGFR and FGFR3 is required in *FGFR3* mutant cancer

A. Western blots of RT112M cells transfected 72 hours earlier with siCON or individual siRNA targeting EGFR (siEGFR-A/B).

B. Growth of RT112M transfected with siCON and two individual siRNA targeting EGFR (A / B) and 48 hours post transfection exposed to a fixed dose of PD173074 (+) or vehicle (-) for 72 hours.

C. Western blot of indicated cell lystates blotted for FGFR3, EGFR, and phosphorylated EGFR, with actin loading control. The three FGFR3 mutant cell lines are indicated.

D. Clonogenic survival assays in indicated cell lines treated continuously with 500nM PD173074, 250nM Gefitinib, the combination, or vehicle alone. *Right*, quantification of three independent experiments.

E. Analysis of S phase fraction from propidium iodidie FACS profiles of indicated cell lines treated for 24 hours with 500nM PD173074, 250nM Gefitinib, combination, or vehicle. * $p<0.05$ Student's T test.

F. Expression of p27 increases with combination therapy at 24 hours, with a minor increase in cleaved PARP in 97-7 cells.

Figure 3. EGFR signalling is upregulated in response to FGFR3 inhibition.

A. Western blot of FGFR3 dependent (RT112M and 639V) and EGFR dependent (97.7 and 94.10) cell lysates treated for the indicated times with 500nM PD173074 blotted for phosphorylated and total EGFR, ERK1/2 and AKT Ser 473.

B. Western blot of RT112M cell lysates treated for the indicated times with 500nM PD173074, 250 nM gefitinib, combination, or vehicle, blotted for phosphorylated and total EGFR and ERK1/2.

C. Clonogenic survival assay of RT112M cells with PD173074 500nM, MEK inhibitor CI-1040 100nM, or the combination. *Right*: quantification of three independent experiments.

D. Western blot of serine 473 phosphorylated and total AKT in RT112M cells treated as indicated.

Figure 4. Mechanism underlying upregulated of EGFR signalling in response to FGFR inhibition.

A. Western blot of RT112M cells treated with PD173074, gefitinib, or CI-1040 100nM as indicated for 6 hours.

B. Western blot of TGFα in RT112M (left) and 97.7 (right) cells treated for indicated times with PD173074, gefitinib, or the combination.

C, Immunofluoresence of RT112M cells treated with 500nM PD170374 for indicated times, or DMSO vehicle, stained for F-actin (red) and EGFR (green).

D. and E. Immunofluoresence of RT112M cells treated with 500nM PD170374 for 4 or 6 hours. D. stained for actin (red) and EGFR (green) and E. at 4 hours stained for EEA1 (red) and EGFR (green).

Figure 5. FGFR3 mediates resistance to EGFR inhibition, with delayed upregulation of FGFR3 signaling resulting from increased FGFR3 transcription.

A. Western blot of partially FGFR3 dependent cell lines (MGHU3, RT112M, 639V) and EGFR dependent cell line (97-7, 94-10) lysates treated for the indicated times with gefitinib.

B and C. Western blot of 97.7 cell lysates treated for the indicated times with PD173074, gefitinib, combination, or vehicle.

D. Western blot of FRS2 following treatment with PD173074, gefitinib or the combination.

E. 97-7 cells were treated with 6 or 24 hours with gefitinib, or DMSO, with quantitative real time RT-PCR assessment FGFR3 mRNA expression expressed relative to expression level in DMSO treated cells.

F. Immunofluoresence of 97-7 cells treated with PD170374 or gefitinib for 24 hours stained for actin (red) and FGFR3 (green)

G. Western blot of cell lystates from *FGFR3* mutant cell lines blotted for FGFR3, EGFR, and actin loading control.

H. Quantitative real time RT-PCR assessment FGFR3 mRNA expression in RT112M and 97.7 cell lines.

Figure 6. Inhibition of EGFR and FGFR3 has combination efficacy *in vivo*

A. RT112M xenografts were established in nude mice, and divided randomly into 4 groups treated with vehicle, PD173074 20mg/mg IP, gefitinib 110mg/kg PO, or combination of both inhibitors for 3 days. Tumour growth was assessed 7 days following commencement of therapy. Comparison between groups with Student's T test.

B. RT112M xenografts were established in nude mice, and divided randomly into 4 groups treated with vehicle, PD173074 15mg/mg IP (days 0-3 and days 7-10), cetuximab 40mg/kg IP (days 0,3,7,10) or combination of both inhibitors with solid bar indicating two week treatment interval. * $p<0.01$ compared to all other groups Student's T test.

C. Kaplan Meier plot of time to tumour doubling from experiment described in part B. Combination treated animals have substantially increased tumour control, $p<0.01$ Log Rank test comparing combination treated animals with all other groups.

D. Expression of TGFα mRNA (TGFA) in a publically available gene expression data set of normal bladder, invasive bladder cancers, and superficial type bladder cancers (36). Comparison between groups with Students T test.

FIGURE 1

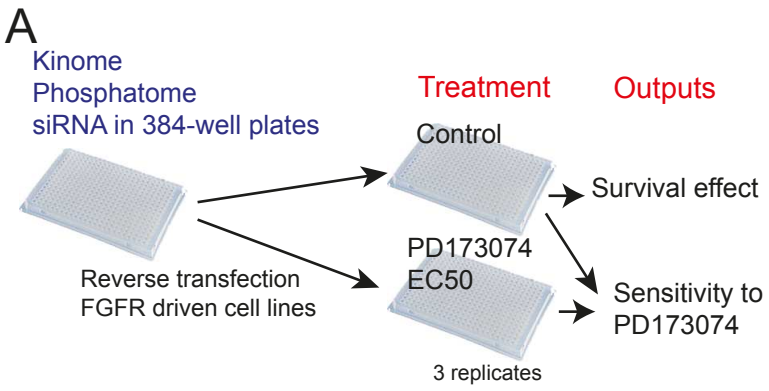
A
Kinome
Phosphatome
siRNA in 384-well plates
Treatment
Outputs
Control
Survival effect
PD173074
EC50
Reverse transfection
FGFR driven cell lines
Sensitivity to
PD173074
3 replicates

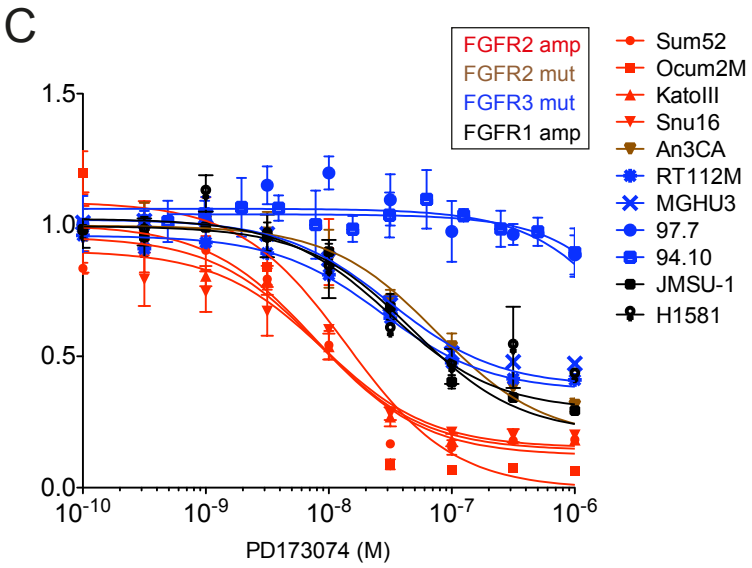
C
FGFR2 amp
FGFR2 mut
FGFR3 mut
FGFR1 amp
Sum52
Ocum2M
KatoIII
Snu16
An3CA
RT112M
MGHU3
97.7
94.10
JMSU-1
H1581
PD173074 (M)

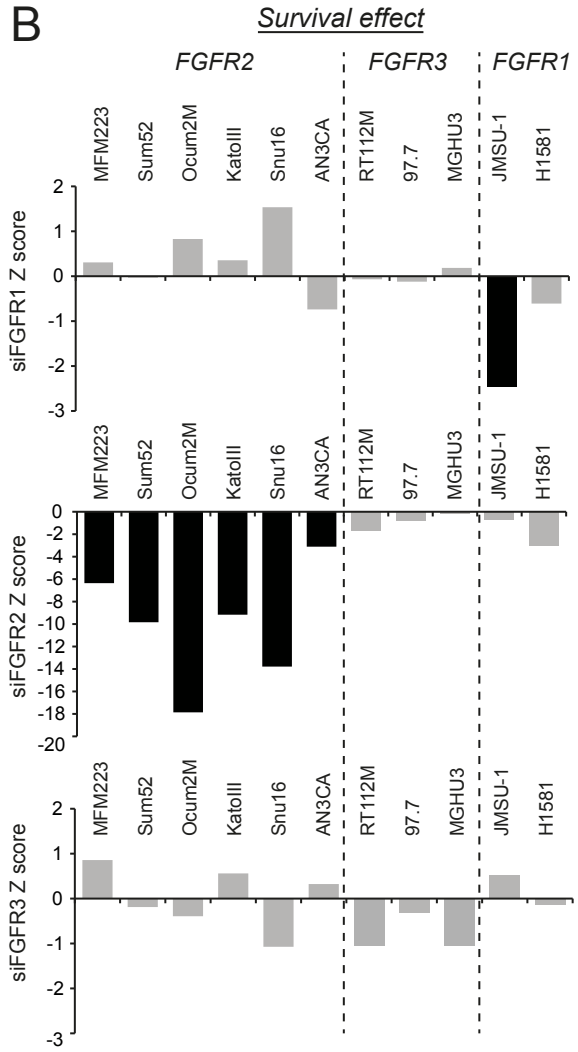
B
Survival effect
FGFR2
FGFR3
FGFR1
siFGFR1 Z score
siFGFR2 Z score
siFGFR3 Z score
MFM223
Sum52
Ocum2M
KatoIII
Snu16
AN3CA
RT112M
97.7
MGHU3
JMSU-1
H1581

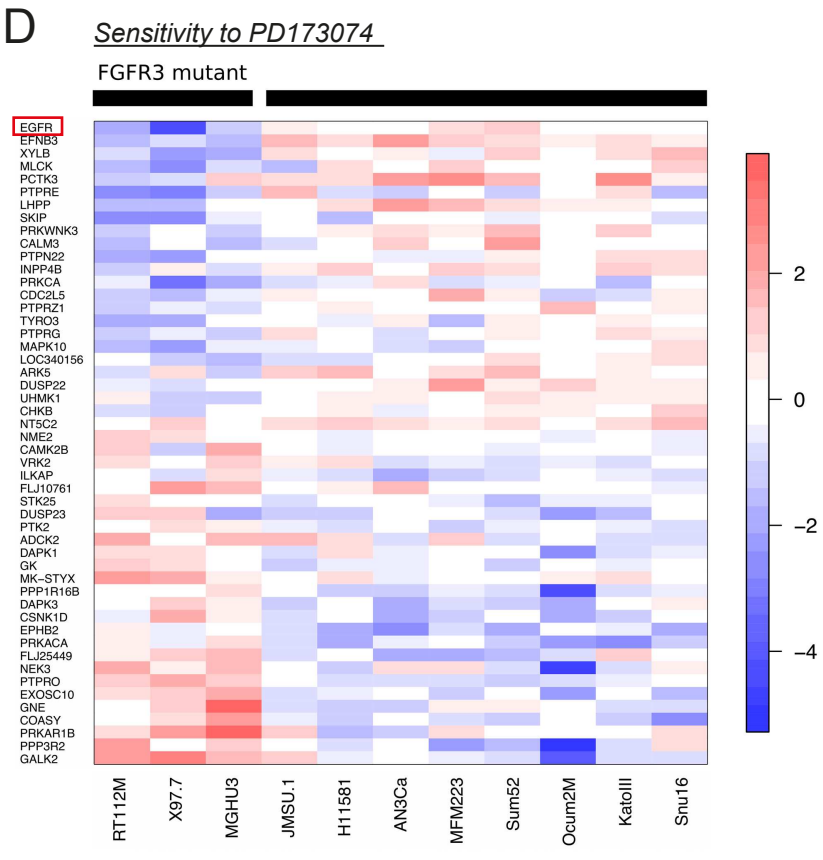
D
Sensitivity to PD173074
FGFR3 mutant
EGFR
RT112M
X97.7
MGHU3
JMSU.1
H11581
AN3Ca
MFM223
Sum52
Ocum2M
KatoIII
Snu16

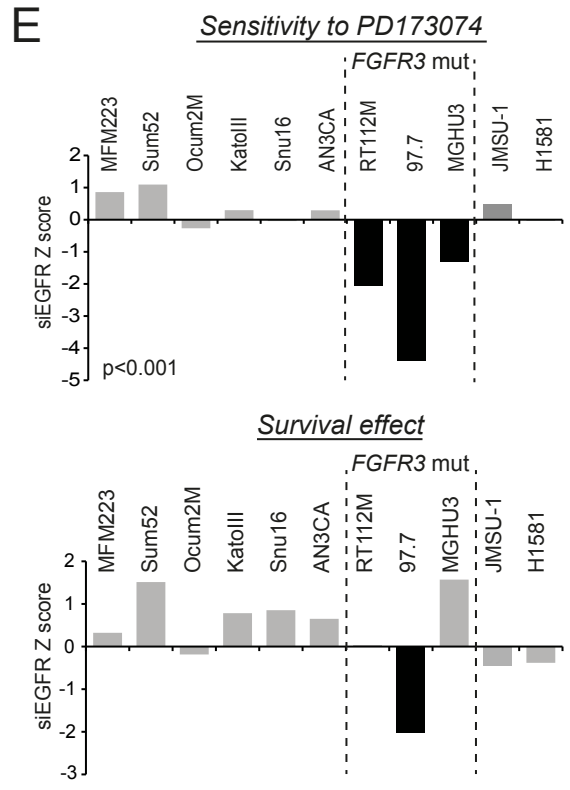
E
Sensitivity to PD173074
FGFR3 mut
siEGFR Z score
p<0.001
Survival effect
FGFR3 mut
siEGFR Z score
MFM223
Sum52
Ocum2M
KatoIII
Snu16
AN3CA
RT112M
97.7
MGHU3
JMSU-1
H1581

FIGURE 2

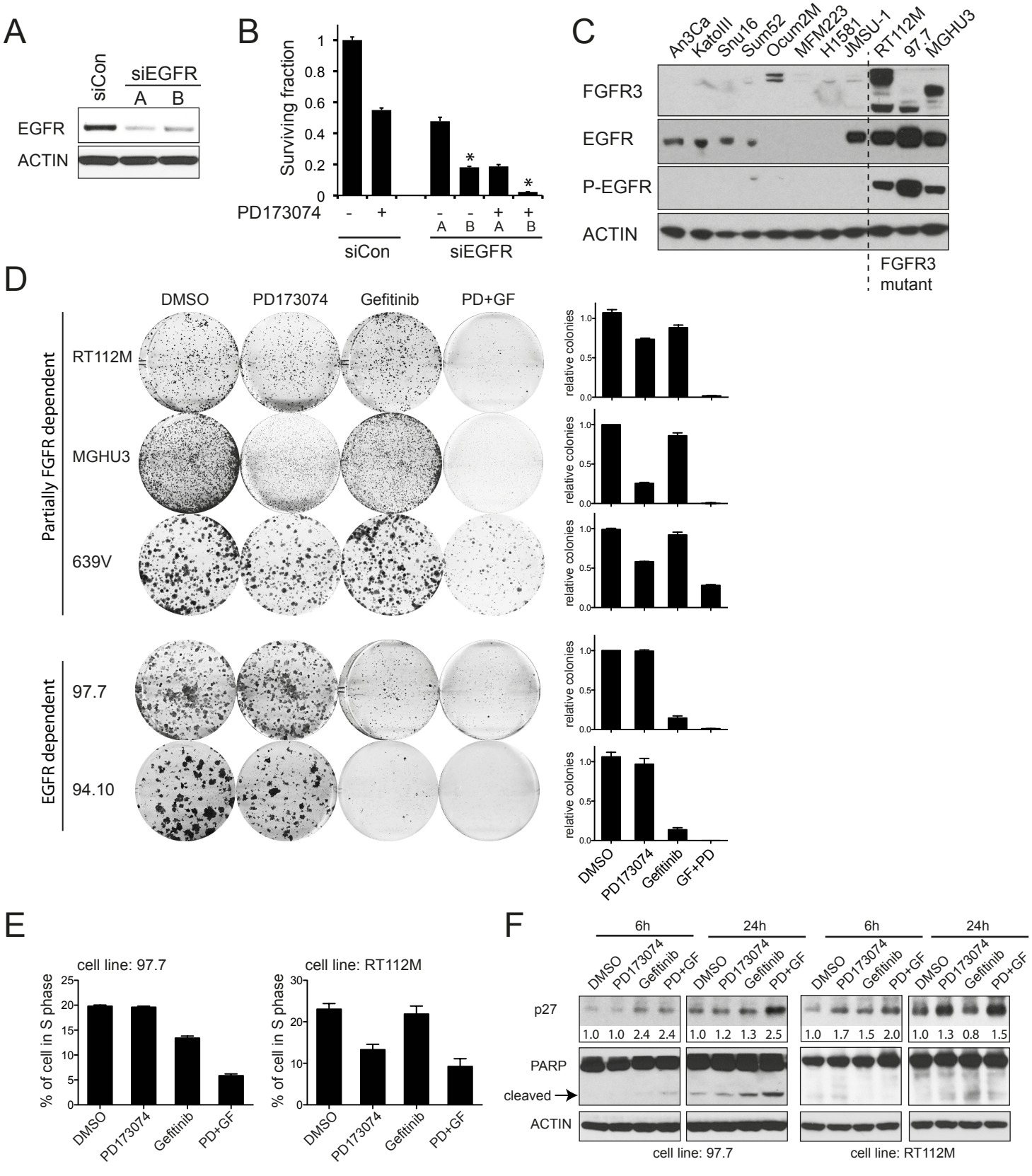
A
siCon
siEGFR
A B
EGFR
ACTIN
B
Surviving fraction
1
0.8
0.6
0.4
0.2
0
PD173074
- + - - + +
A B A B
siCon
siEGFR
C
An3Ca KatoIII Snu16 Sum52 Ocum2M MFM223 H1581 JMSU-1 RT112M 97.7 MGHU3
FGFR3
EGFR
P-EGFR
ACTIN
FGFR3 mutant
D
DMSO PD173074 Gefitinib PD+GF
Partially FGFR dependent
RT112M
MGHU3
639V
EGFR dependent
97.7
94.10
relative colonies
1.0
0.5
0.0
DMSO PD173074 Gefitinib GF+PD
E
cell line: 97.7
cell line: RT112M
% of cell in S phase
25
20
15
10
5
0
30
DMSO PD173074 Gefitinib PD+GF
F
6h 24h 6h 24h
DMSO PD173074 Gefitinib PD+GF
p27
1.0 1.0 2.4 2.4
1.0 1.2 1.3 2.5
1.0 1.7 1.5 2.0
1.0 1.3 0.8 1.5
PARP
cleaved
ACTIN
cell line: 97.7
cell line: RT112M

FIGURE 3

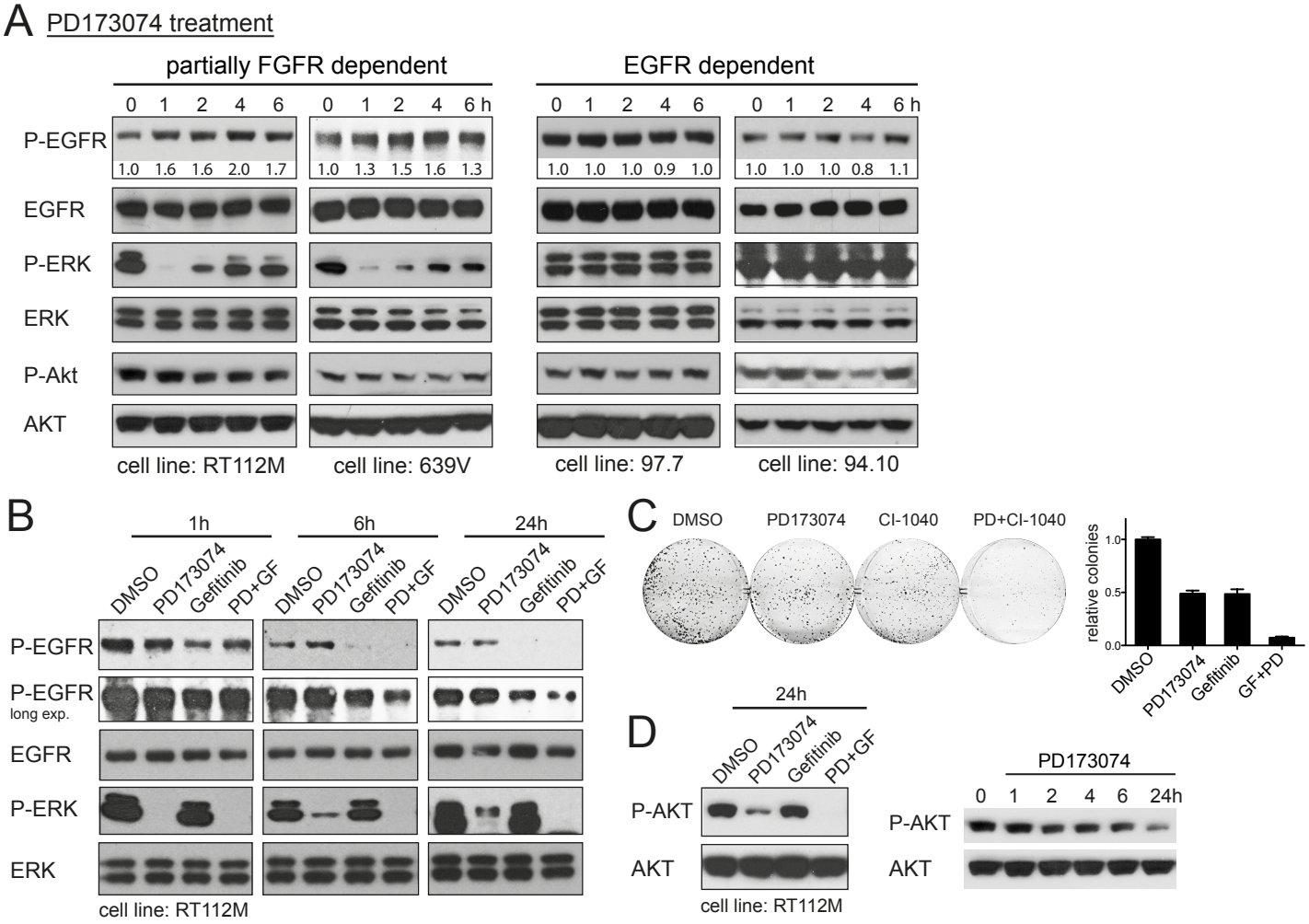
A PD173074 treatment
partially FGFR dependent
EGFR dependent
0 1 2 4 6 0 1 2 4 6 h
0 1 2 4 6 0 1 2 4 6 h
P-EGFR
1.0 1.6 1.6 2.0 1.7
1.0 1.3 1.5 1.6 1.3
1.0 1.0 1.0 0.9 1.0
1.0 1.0 1.0 0.8 1.1
EGFR
P-ERK
ERK
P-Akt
AKT
cell line: RT112M
cell line: 639V
cell line: 97.7
cell line: 94.10
B
1h
6h
24h
DMSO
PD173074
Gefitinib
PD+GF
P-EGFR
P-EGFR
long exp.
EGFR
P-ERK
ERK
cell line: RT112M
C
DMSO
PD173074
CI-1040
PD+CI-1040
relative colonies
1.0
0.5
0.0
DMSO
PD173074
Gefitinib
GF+PD
D
24h
DMSO
PD173074
Gefitinib
PD+GF
P-AKT
AKT
cell line: RT112M
PD173074
0 1 2 4 6 24h
P-AKT
AKT

FIGURE 4

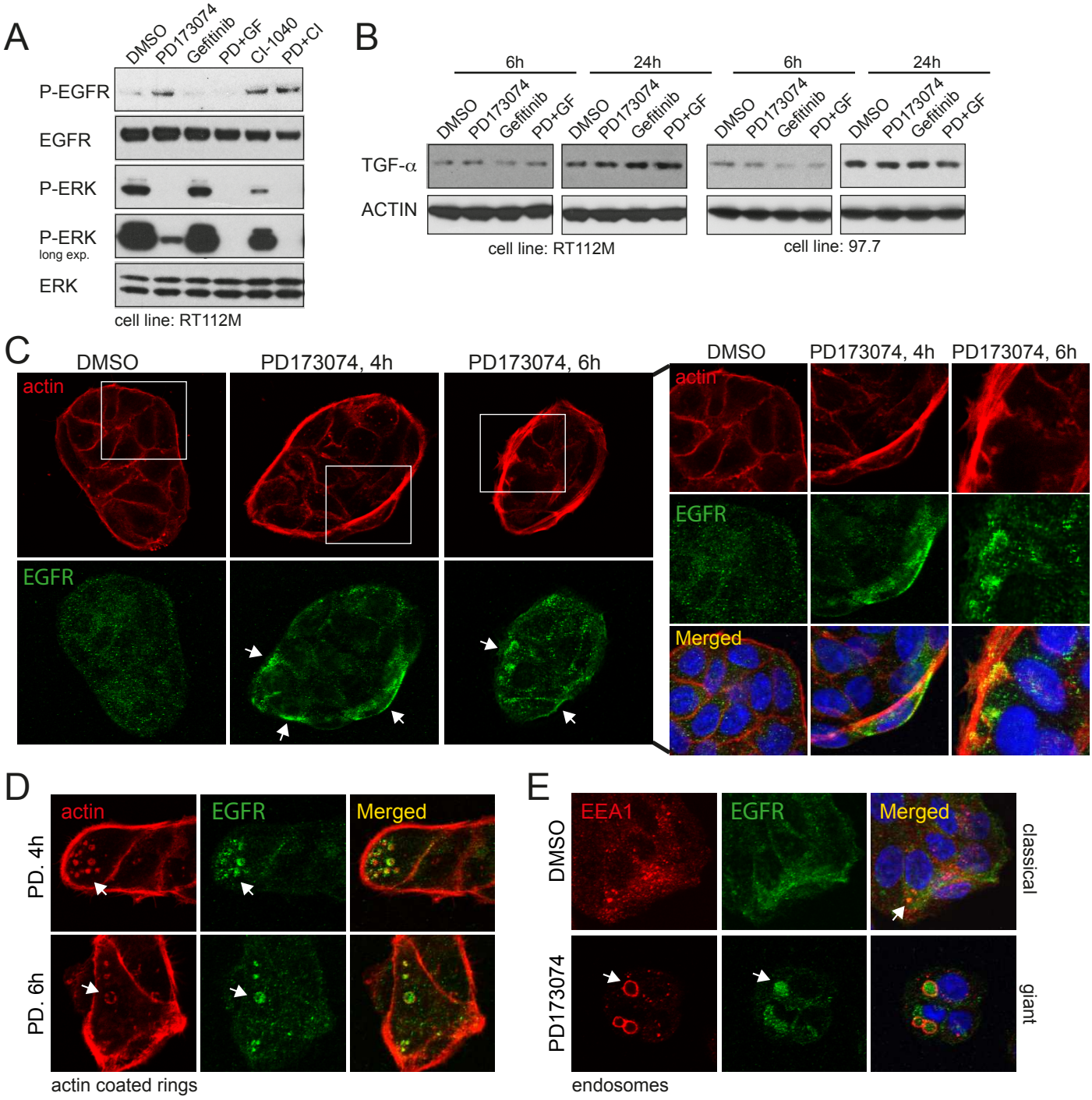
A
DMSO
PD173074
Gefitinib
PD+GF
CI-1040
PD+CI
P-EGFR
EGFR
P-ERK
P-ERK
long exp.
ERK
cell line: RT112M
B
6h
24h
6h
24h
DMSO
PD173074
Gefitinib
PD+GF
TGF-α
ACTIN
cell line: RT112M
cell line: 97.7
C
DMSO
PD173074, 4h
PD173074, 6h
actin
EGFR
Merged
D
PD. 4h
PD. 6h
actin
EGFR
Merged
actin coated rings
E
DMSO
PD173074
EEA1
EGFR
Merged
classical
giant
endosomes

FIGURE 5

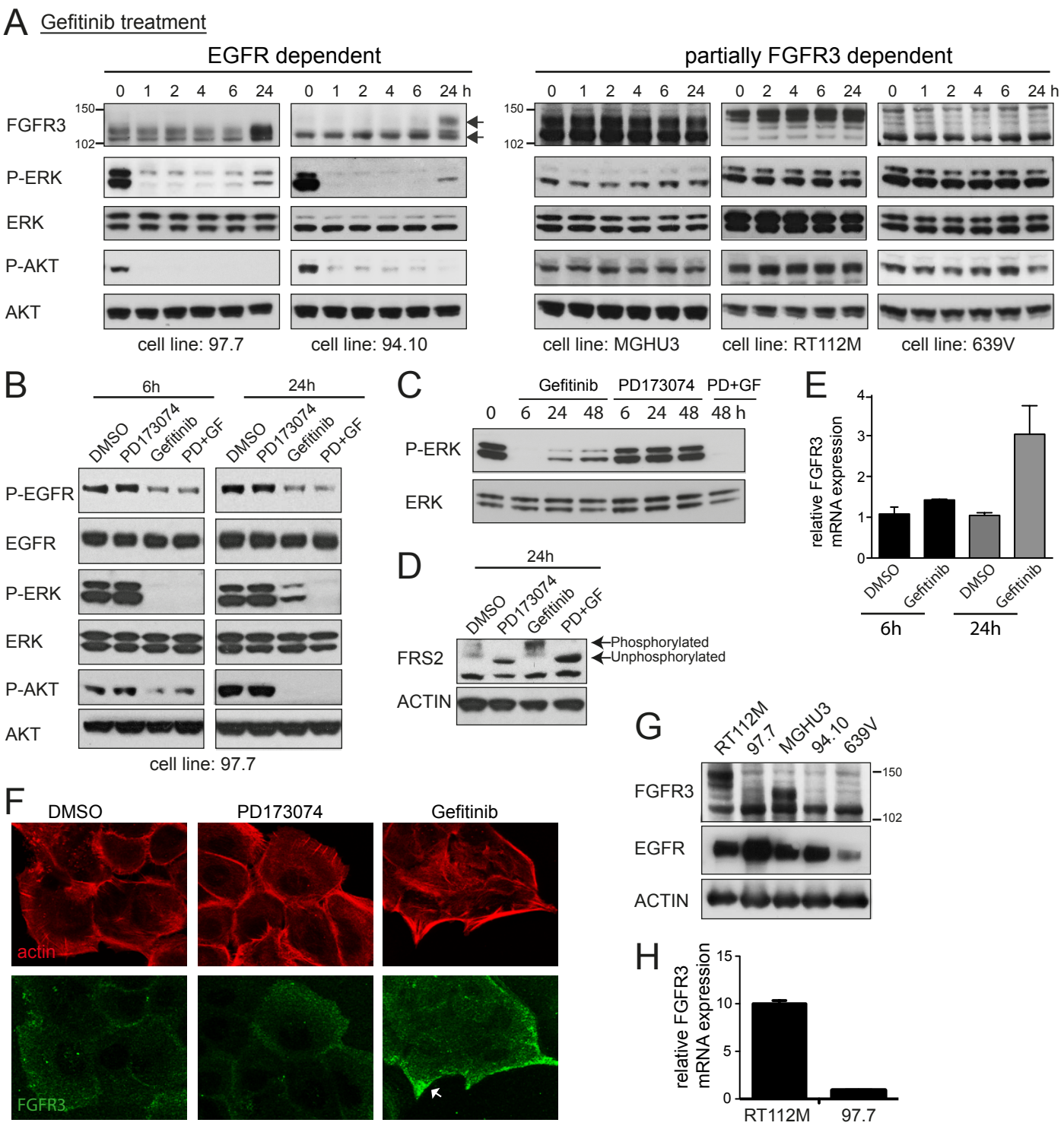
A Gefitinib treatment
EGFR dependent
partially FGFR3 dependent
0 1 2 4 6 24 0 1 2 4 6 24 h
0 1 2 4 6 24 0 2 4 6 24 0 1 2 4 6 24 h
150
102
FGFR3
P-ERK
ERK
P-AKT
AKT
cell line: 97.7
cell line: 94.10
cell line: MGHU3
cell line: RT112M
cell line: 639V
B
6h
24h
DMSO
PD173074
Gefitinib
PD+GF
P-EGFR
EGFR
P-ERK
ERK
P-AKT
AKT
cell line: 97.7
C
Gefitinib
PD173074
PD+GF
0 6 24 48 6 24 48 48 h
P-ERK
ERK
D
24h
DMSO
PD173074
Gefitinib
PD+GF
FRS2
Phosphorylated
Unphosphorylated
ACTIN
E
relative FGFR3 mRNA expression
0
1
2
3
4
DMSO
Gefitinib
DMSO
Gefitinib
6h
24h
F
DMSO
PD173074
Gefitinib
actin
FGFR3
G
RT112M
97.7
MGHU3
94.10
639V
FGFR3
150
102
EGFR
ACTIN
H
relative FGFR3 mRNA expression
0
5
10
15
RT112M
97.7

FIGURE 6

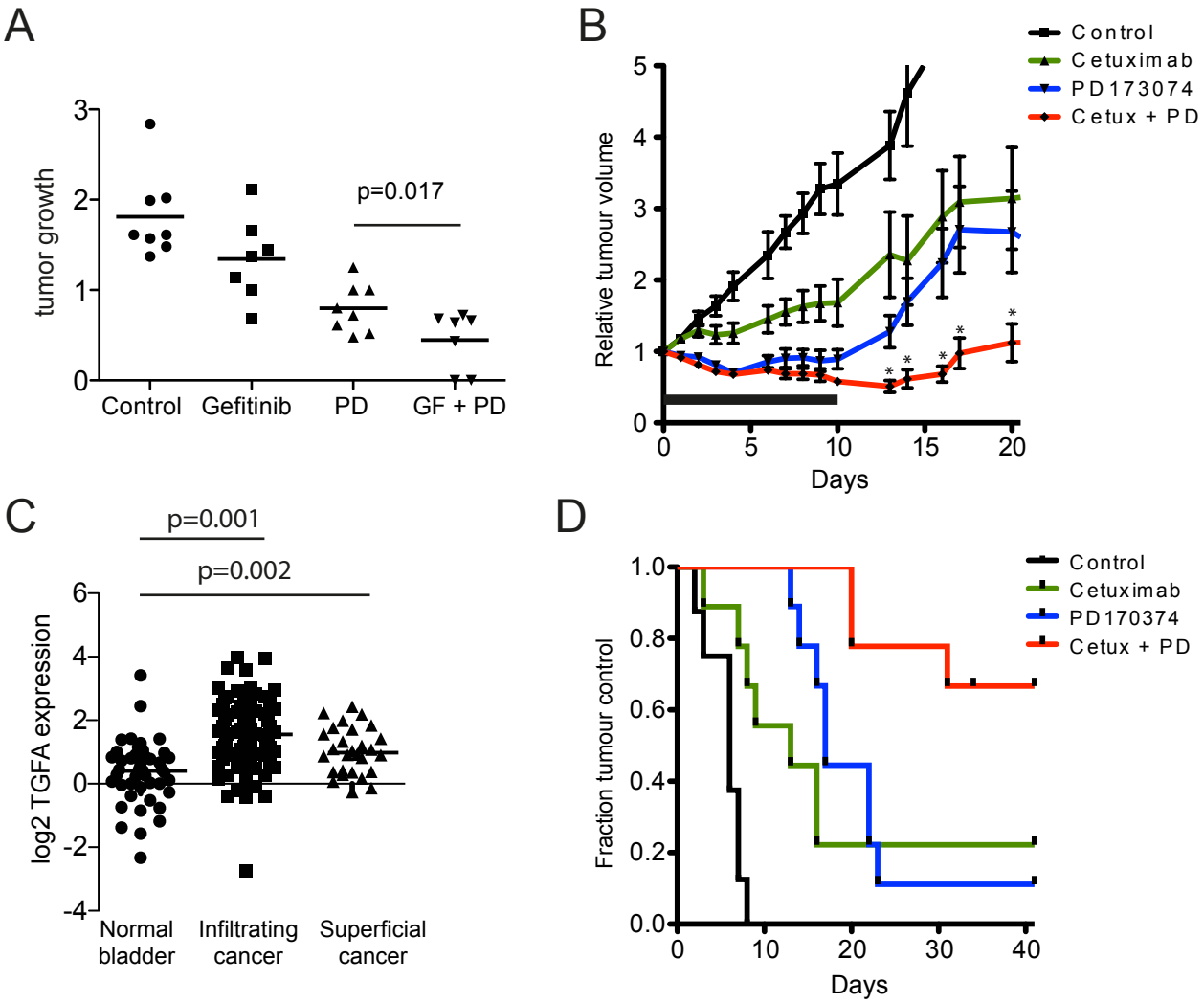
A
tumor growth
p=0.017
Control
Gefitinib
PD
GF + PD
B
Relative tumour volume
Days
Control
Cetuximab
PD173074
Cetux + PD
C
log2 TGFA expression
p=0.001
p=0.002
Normal bladder
Infiltrating cancer
Superficial cancer
D
Fraction tumour control
Days
Control
Cetuximab
PD170374
Cetux + PD